JOURNAL OF NANO- AND ELECTRONIC PHYSICS
Vol. 18 No 3, 03013(5pp) (2026)
ЖУРНАЛ НАНО- ТА ЕЛЕКТРОННОЇ ФІЗИКИ
Том 18 № 3, 03013(5cc) (2026)

REGULAR ARTICLE

Development of a Gigahertz-Range Microstrip Sensor for Monitoring the Doping of Semiconductor Structures

R.S. Chykun* ✉, I.M. Bondarenko, O.V. Hlukhov, V.A. Chekubasheva

Kharkiv National University of Radio Electronics, 61166 Kharkiv, Ukraine

(Received 15 March 2026; revised manuscript received 21 June 2026; published online 26 June 2026)

The work presents the concept of a microstrip resonant sensor designed for non-destructive monitoring of dopant concentration in semiconductor structures. The sensor architecture is based on two coupled microstrip lines with a localized electric field in a narrow slot, which ensures high sensitivity to variations in effective permittivity and intrinsic material losses. A full-wave simulation was performed in Ansys HFSS to analyze the device operation, accurately reproducing the actual geometry and physical parameters of the sensor, the properties of the Rogers RO3003 substrate, and the characteristics of the inserted sample.

Three slot-filling conditions were investigated: air, monocrystalline silicon, and doped silicon with an increased concentration of free carriers. It is shown that introducing silicon shifts the resonance frequency toward lower values due to the increased effective permittivity, while doping further reduces the quality factor and broadens the $|S_{12}|$ ($|S_{21}|$) resonance dip as a result of higher electromagnetic losses. The obtained S-parameter responses confirm the capability of the sensor to distinguish materials with closely spaced parameters and to determine the doping level based on frequency shift and quality-factor degradation. The proposed structure demonstrates high sensitivity and reproducibility and can be employed for rapid non-destructive testing of silicon materials in the gigahertz range as well as for further integration into mass production.

Keywords: Microstrip lines, Dielectric permittivity, Doped semiconductors, Slot structures, Resonance, Dielectric substrates.

DOI: 10.21272/jnep.18(3).03013 PACS numbers: 84.40. – x, 07.57.kp

1. INTRODUCTION

Assessing the concentration of impurities in semiconductor materials is a critically important step in controlling technological processes and forming the electrical parameters of devices. Traditional analysis methods, in particular SIMS and C-V profiling, provide high accuracy in determining the impurity profile, but SIMS remains destructive and requires complex laboratory infrastructure, while C-V methods, although less demanding, they are only applicable to specially prepared test structures [1-3]. This has led to growing interest in non-destructive, non-contact approaches capable of establishing a connection between the dielectric properties of a material and its doping level in the microwave range, where changes in electrophysical parameters are most sensitive [4, 5].

In this context, microstrip resonant structures are a promising platform for local assessment In this context, microstrip resonant structures are a promising platform for local assessment of complex dielectric permittivity $\varepsilon^*(\omega)$ and related impurity concentrations. The concentration of free carriers N directly affects the resonance frequency and quality factor, which allows obtaining informative parameters without disturbing the integrity of the sample. Recent studies demonstrate the effectiveness of dielectric spectroscopy and S- parameter analysis methods for determining material parameters [6-9], as well as the success of various types of microstrip and planar sensors – based on coupled resonators, split-ring structures, and their modifications – for highly sensitive measurement of ε and anisotropy [4, 5, 10-16].

Despite significant progress, most approaches require complex numerical modeling, multi-step calibration, or precise specification of geometric and material parameters. This limits the ability to quickly and accurately determine dielectric characteristics related to the concentration of dopant impurities. Therefore, there is a pressing need to develop a microstrip microwave sensor that allows for the interpretation of measured S_{11} and S_{21} values while maintaining high sensitivity to changes in doping parameters.

2. SENSOR DESIGN

The proposed sensor structure is implemented in the form of two parallel microstrip lines on a low-loss dielectric substrate. The conductors form a system of coupled lines, the parameters of which are selected so as to ensure the excitation of a paired resonant mode when energy is supplied through external ports. This approach allows the formation of stable resonance characteristics that are sensitive to changes in effective electromagnetic parameters in the interaction zone [5, 15].

An elongated slit is formed between the microstrip conductors, which serves as a landing place for the

* Correspondence e-mail: roman.chykun@nure.ua

© 2026 The Author(s). Journal of Nano- and Electronic Physics published by Sumy State University. This article is distributed under the terms and conditions of the Creative Commons Attribution (CC BY) license.

Cite this article as: R.S. Chykun et al., *J. Nano- Electron. Phys.* 18 No 3, 03013 (2026) https://doi.org/10.21272/jnep.18(3).03013

semiconductor material under study. The geometric dimensions of the slit are selected so as to ensure a fixed and reproducible position of the sample, since the gap extends along the entire central part of the sensor and has no pronounced geometric restrictions in the longitudinal direction, the position of the sample is determined mainly by its transverse dimensions and the electrodynamic conditions of interaction with the field, rather than by mechanical fixation. The thickness of the sample must correspond to the width of the slit, which ensures the placement of the material in the area of maximum electric field concentration and the reproducibility of measurements.

Placing the sample in the gap allows it to be positioned at the maximum of the electric field. This, in turn, allows significant local sensitivity to be achieved even to minor changes in the permeability or internal losses of the semiconductor. [4, 11].

Two TEM-type microwave ports connected to the ends of microstrip lines are used to input the signal. This configuration of connection lines ensures symmetrical excitation of the structure and minimizes parasitic modes, allowing for a clear resonant response. The ports are located on the extension of the microstrip lines, which ensures symmetrical excitation of the structure and reproducibility of results when analyzing its frequency characteristics.

The microstrip design of the sensor ensures its compatibility with standard printed circuit board technologies, high accuracy of geometry reproduction, and the ability to scale parameters for different frequency ranges. The resonant properties of the structure are determined by the configuration of the connected lines and the dielectric characteristics of the substrate, so the sensor does not require additional tuning after manufacture.

Optimization of the geometry of all elements – connected lines, sample slots, and input ports – is aimed at obtaining the maximum difference in resonance characteristics when changing the parameters of the material placed in the slot. This makes the sensor an effective tool for non-destructive analysis of semiconductor structures in the gigahertz range [10].

3. SENSOR OPERATING PRINCIPLE

The sensor operates based on the excitation of a paired mode in a system of two connected microstrip lines [4]. In this mode, the currents in the conductors are symmetrical, resulting in the dominance of the normal component of the electric field relative to the substrate. It is this field region that determines the sensitivity of the structure to changes in the electromagnetic parameters of the material placed in the gap.

In the absence of a sample, the resonant frequency and quality factor of the resonator are determined by the geometry of the connected lines and the properties of the substrate. After introducing a semiconductor material into the gap, interaction with the vertical field occurs, which changes the conditions for energy accumulation in the resonant volume and the level of internal losses in the sample [5]. This leads to a shift in the resonant frequency and a change in the quality factor, which serve as informative parameters for evaluating the electromagnetic characteristics of the sample.

Thus, the properties of the material are determined by changes in the position and shape of the resonance dip in the S-parameters, which allows analyzing both polarization and dissipative processes in the gigahertz range [16]. The theory of the dependence of these parameters on the doping concentration is being studied separately.

4. MODELING METHODOLOGY

To verify the proposed method, a full-wave model of a microstrip sensor was created in the Ansys HFSS (High Frequency Structure Simulator) software environment. The substrate was made of Rogers RO3003 [17] material with a thickness of 0.5 mm, and the conductors were made of copper. The overall dimensions of the sensor were 21 × 32 mm. The microstrip lines were 1.27 mm wide and 12.725 mm long, and the port connection lines were 8.44 mm long with a 0.3 mm gap between the port and the line. The slot for installing the sample was 1 mm wide, 0.17 mm deep, and 32 mm long. Samples of semiconductor materials were specified in the form of parallelepipeds with dimensions 32 × 0,8 × 3 mm. The external appearance of the sensor is shown in Fig. 1.

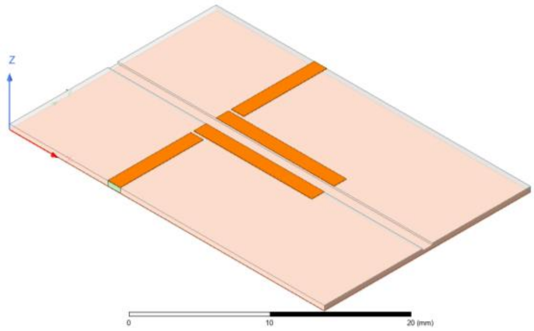

Fig. 1 – Sensor model

The model included two coupled microstrip lines and a slot for material placement, and the excitation ports were tuned as ideal TEM inputs with a wave impedance of 50 ohms. In HFSS, the frequency dependence of the *S*-parameters was calculated in the range covering the resonant modes of the sensor.

The resonance perturbation method [6] was used for measurements, which allows determining the complex dielectric permeability of the material through the shift of the resonance frequency and quality factor. The main measured parameters are frequency f and quality factor Q. Complex permeability is described as: $\varepsilon_r(\omega) = \varepsilon_r'(\omega) - j\varepsilon_r''(\omega)$, де ε_r' – real component (dielectric constant), and ε_r'' – imaginary component (electrical absorption).

Three states of the gap were considered, which made it possible to evaluate the influence of the material without additional parameter variations:

- air – reference configuration.
- silicon – basic dielectric state.
- doped silicon – material with modified electromagnetic properties.

For each state in HFSS, frequency dependencies are formed $|S_{21}|$, which were used to determine the resonance parameters. This made it possible to evaluate the sensor's response to changes in material properties and confirmed the suitability of the structure for studying semiconductors in the gigahertz range.

During modeling, the impact of concentration profile variations was assessed. $N(x)$ resonant frequencies and quality factors. The actual dielectric properties of the substrate and conductors, as well as the geometry of the gap, were taken into account.

5. RESULTS

During modeling, the sensor was studied in three main states: in the reference version without a sample, when the gap between the microstrip lines is filled with air; in a configuration with a single-crystal silicon sample; and in conditions when silicon with an increased concentration of free carriers is located in the gap. This approach made it possible to consistently evaluate the influence of the material on the resonance characteristics and determine the degree of sensitivity of the sensor to changes in dielectric and dissipative properties.

1. Air (reference condition)

Filling the gap with air (Table 1) ensured a stable resonance response, which was determined only by the parameters of the substrate and conductors. At the resonance point, the minimum $|S_{21}|$ was accompanied by a high resonance response quality factor of $\boldsymbol{Q} = \mathbf{239.15}$. This state was used as a reference for further comparison.

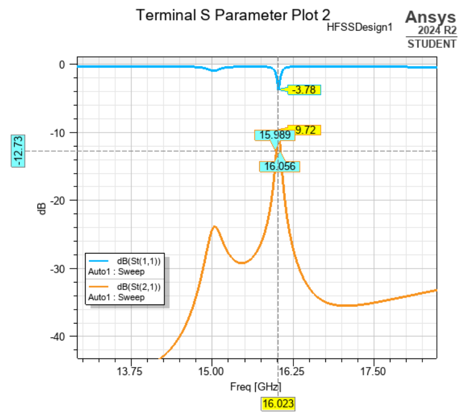

Fig. 2 – $|S_{11}|$ and $|S_{21}|$ for a sensor without a sample

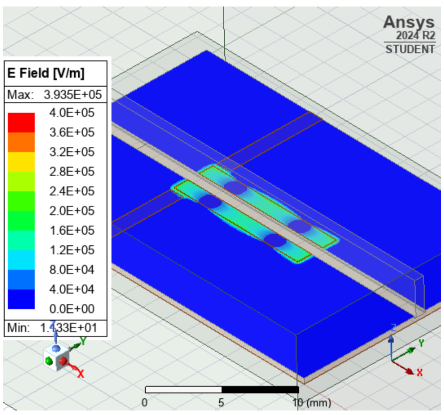

Fig. 3 – Distribution of electric field intensity for the sensor when the gap is filled with air

Table 1 – Basic parameters of samples in Ansys HFSS environment

Parameters Ansys HFSS \ Sample	Air	Silicon	Doped Silicon
Relative Permittivity	1.0006	11.9	11.9
Relative Permeability	1.0000004	1	1
Bulk Conductivity	0	0	1

2. Silicon (undoped)

The introduction of single-crystal silicon (Table 1) led to a shift in the resonance frequency toward lower values from 16,023 GHz to 15.365 GHz which is due to an increase in the effective dielectric permeability in the gap region. The change in resonance quality factor, which was $\boldsymbol{Q} = \mathbf{284,54}$, reflects a decrease in effective dielectric losses in the material.

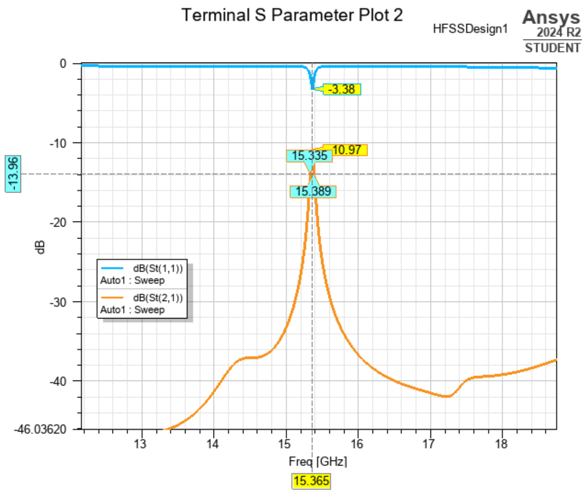

Fig. 4 – $|S_{11}|$ and $|S_{21}|$ for a sensor with a gap filled with a sample of its own silicon

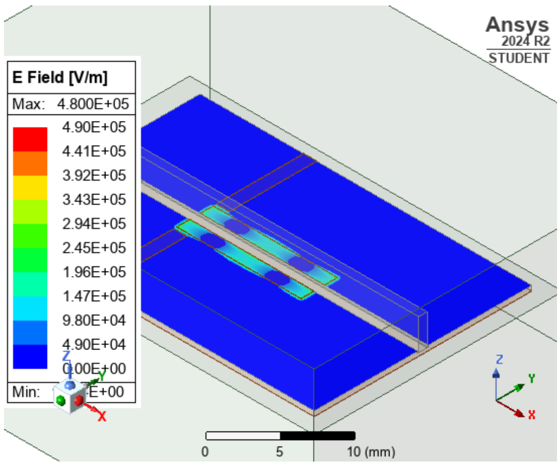

Fig. 5 – Distribution of electric field intensity for the sensor when filling the gap with a sample of pure silicon

3. Doped silicon

In the presence of free charge carriers, a change in the resonant response of the sensor was observed without a shift in the resonant frequency, as well as a change in the width of the minimum of the transmission coefficient modulus. $|S_{21}|$. The resonance quality factor decreased and amounted to $\boldsymbol{Q = 146.33}$, which is associated with an increase in conduction losses in doped silicon (Table 1). The magnitude of the decrease in quality factor exceeded the corresponding changes for undoped silicon, indicating the sensitivity of the sensor structure to variations in electromagnetic parameters caused by the presence of free charge carriers.

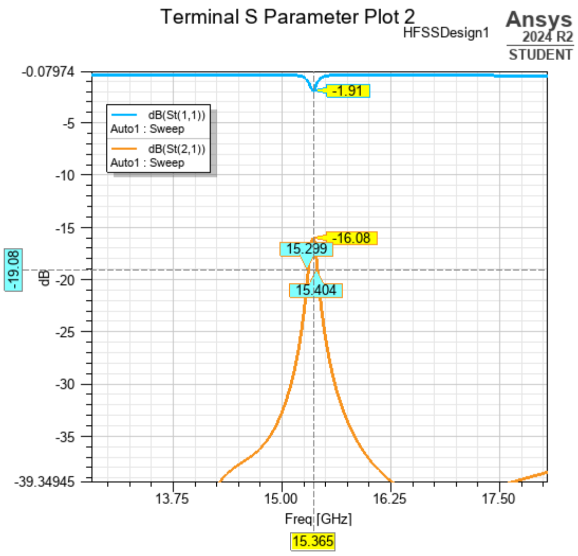

Fig. 6 – $|S_{11}|$ and $|S_{21}|$ for a sensor with a doped cream sample

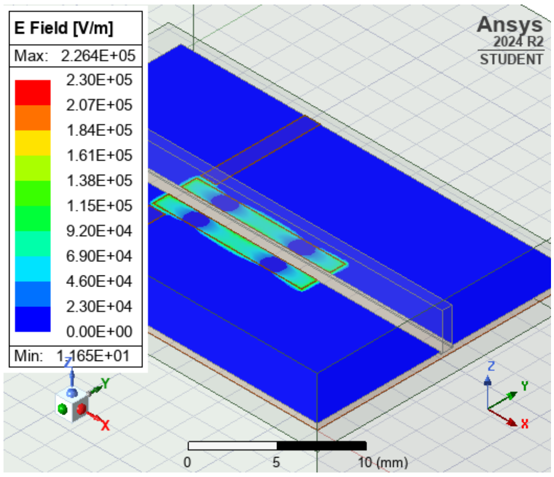

Fig. 7 – Electric field distribution for a sensor with a doped silicon sample

A comparison of the three states considered showed a consistent increase in the influence of the material on the resonance characteristics during the transition from air filling to single-crystal silicon and the subsequent use of doped silicon, which corresponds to an increase in effective dielectric permeability and total electromagnetic losses in the field localization zone. This behavior indicates the sensor's ability to distinguish between materials with similar electrophysical parameters and respond to changes in charge carrier concentration, which is a necessary condition for the implementation of non-destructive analysis of semiconductor structures.

The HFSS results confirmed the high sensitivity of the sensor to local changes in permeability and its suitability for reconstructing the $N(x)$ profile in semiconductor materials with a spatial impurity gradient.

6. CONCLUSIONS

During the study, frequency characteristics of the microstrip sensor were obtained, which demonstrate a clear dependence on the electrophysical parameters of the material in the gap area. The transition from air to silicon is accompanied by a shift of the resonance frequency to the lower part of the spectrum, which confirms the ability of the structure to respond accurately to changes in dielectric permeability.

Analysis of the sensor behavior with silicon samples of different doping levels showed a significant difference in the shape of the spectral curve. Doped silicon causes an increase in electromagnetic losses, which manifests itself in a decrease in quality factor and a broadening of the resonance peak. As the carrier concentration increases, additional suppression of the resonance amplitude is observed, which is due to an increase in the conductivity of the material and increased losses in the substrate. This effect allows materials to be distinguished not only by their dielectric constant, but also by their level of internal conductivity, which is critically important for assessing the degree of doping.

The sensor demonstrates stability and reproducibility of response for all considered sample variants, confirming the effectiveness of the resonant approach for non-destructive diagnostics of semiconductor structures. The sensitivity of the design to the parameters of the analyzed sample opens up the possibility of its use in technological control, quality monitoring, and research of heterogeneous materials.

The configuration based on two connected open microstrip lines provides effective localization of the electric field and a high degree of interaction with the sample, which makes such a structure promising for practical implementation of research in the gigahertz range. The set of results obtained forms the scientific basis for the development of microstrip sensor systems for fast and accurate control of the doping level of semiconductor structures.

REFERENCES

1. M.-A. Pinault-Thaury, F. Jomard, *Mater. Sci. Forum Submitted* **1062**, 376 (2022) https://doi.org/10.4028/p-684nsi.
2. J. Zheng, Y. Zhang, Y. Zhou, L. Lin, Y. Zhang, *Sci. Bull.* **65**, 161 (2019) https://doi.org/10.1016/j.scib.2019.11.001.
3. Z. Khosravizadeh, M. Trzyna-Sowa, A. Lysak, E. Przezdziecka, R. Jakiela, *J. Phys. D: Appl. Phys.* **58** 025303 (2025) https://doi.org/10.1088/1361-6463/ad80a0.
4. H. Morales-Lovera, J.-L. Olvera-Cervantes, A.-E. Perez-Ramos, A. Corona-Chavez, C.E. Saavedra, *Sci. Rep.* **12**, 2205 (2022) https://doi.org/10.1038/s41598-022-06259-8.
5. H. Morales-Lovera, J.-L. Olvera-Cervantes, A. Corona-Chavez, T.K. Kataria, *IEEE Trans. Microw. Theory Techn.* **68**, 1610 (2020) https://doi.org/10.1109/TMTT.2019.2958265.
6. L. Chen, C.K. Ong, B.T.G. Tan, *IEEE Trans. Instrum.*

Meas. **48**, 1023 (1999) https://doi.org/10.1109/19.816108.
7. P.I. Dankov, *IEEE Trans. Microw. Theory Techn.* **54**, 1534 (2006) https://doi.org/10.1109/TMTT.2006.871247.
8. J. Krupka, A. Pacewicz, P. Kopyt, B. Salski, *Mater. Res. Bull.* **179**, 112994 (2024) https://doi.org/10.1016/j.materresbull.2024.112994.
9. T. Yamaguchi, N. Yamamoto, D. Naito, T. Takahashi, S. Sakanaka, *Nucl. Instrum. Meth. Phys. Res. Sect. A* **1064**, 169449 (2024) https://doi.org/10.1016/j.nima.2024.169449.
10. S. Ahmadi, J.-L. Olvera-Cervantes, H. Morales-Lovera, C.E. Saavedra, *IEEE Access* **4**, 1 (2022).
11. H. Morales-Lovera, J.-L. Olvera-Cervantes, A.-E. Perez-Ramos, A. Corona-Chavez, C.E. Saavedra, *IEEE Access* **11**, 39418 (2023) https://doi.org/10.1109/ACCESS.2023.3322973.
12. M.A.M. Said, Z. Zakaria, M.H. Misran, M.A. Othman, R.A. Manap, A.S. Jaafar, S. Suhaimi, N.I. Hassan, *EMITTER Int. J. Eng. Technol.* **11** No 1, 60 (2023).
13. H.-Y. Gan, W.-S. Zhao, Q. Liu, D.-W. Wang, L. Dong, G. Wang, W.-Y. Yin, *IEEE Sens. J.* **20** No 11, 5876 (2020) https://doi.org/10.1109/JSEN.2020.2973196.
14. K. Masrakin, S.Z. Ibrahim, H.A. Rahim, S.N. Azemi, P.J. Soh, S. Tantiviwat, *Micromachines* **14**, 790 (2023) https://doi.org/10.3390/mi14040790.
15. L.-V. Herrera-Sepulveda, J.-L. Olvera-Cervantes, A. Corona-Chavez, T. Kaur, *IEEE Microwave Wireless Compon. Lett.* **29** No 9, 626 (2019) https://doi.org/10.1109/LMWC.2019.2928295.
16. C. Liu, C. Liao, Y. Peng, W. Zhang, B. Wu, P. Yang, *Sensors* **24**, 7696 (2024) https://doi.org/10.3390/s24237696.
17. Rogers Corporation, RO3000® Series Circuit Materials, https://www.rogerscorp.com//media/project/rogerscorp/documents/advanced-electronics-solutions/english/data-sheets/ro3000-laminate-data-sheet-ro3003----ro3006----ro3010----ro3035.pdf (2016).

Створення мікросмужкового сенсора гігагерцового діапазону для контролю легування напівпровідникових структур

Р.С. Чикун, І.М. Бондаренко, О.В. Глухов, В.А. Чекубашева

Харківський національний університет радіоелектроніки, 61166 Харків, Україна

У роботі представлено концепцію мікросмужкового резонансного сенсора, який призначений для неруйнівного контролю концентрації домішок у напівпровідникових структурах. Конструкція сенсора побудована на двох зв'язаних мікросмужкових лініях з локалізованим електричним полем у вузькій щілині, що забезпечує високу чутливість до зміни ефективної діелектричної проникності та внутрішніх втрат матеріалу. Для аналізу роботи пристрою виконано повнохвильове моделювання в програмному середовищі Ansys HFSS, у якому відтворено реальну геометрію та фізичні параметри сенсора, параметри підкладки Rogers RO3003 та характеристики введеного зразка.

Досліджено три стани заповнення щілини: повітрям, монокристалічним кремнієм та легованим кремнієм з підвищеною концентрацією вільних носіїв. Показано, що введення кремнію спричиняє зсув резонансної частоти у нижчу область спектра через збільшення ефективної проникності, а присутність легування додатково знижує добротність та розширює резонансний провал $|S_{21}|$ внаслідок зростання електромагнітних втрат. Отримані залежності S-параметрів підтверджують здатність використання сенсора для розрізнення матеріали з близькими параметрами та визначення рівню легування за характером зміщення частоти й зміною добротності. Запропонована структура демонструє високу чутливість та відтворюваність і може бути використана для швидкого неруйнівного контролю кремнієвих матеріалів у гігагерцовому діапазоні а також бути впроваджена в серійне виробництво.

Ключові слова: Мікросмужкові лінії, Діелектрична проникність, Леговані напівпровідники, Щілини, Резонанс, Діелектричні підкладки.